

Supplementary Materials of

Parameterized reactivity of hydroxy radical, ozone, nitrate radical and atmospheric oxidation capacity during summer at a suburban site between Beijing and Tianjin

Yuan Yang^{1,2}, Yonghong Wang³, Dan Yao^{1,2,6}, Dongsheng Ji¹, Jie Sun¹, Yinghong Wang¹, Shuman Zhao^{1,2}, Wei Huang^{1,2}, Shuanghong Yang^{1,5}, Wenkang Gao¹, Zirui Liu¹, Bo Hu¹, Renjian Zhang¹, Limin Zeng⁴, Tuukka Petäjä³, Veli-Matti Kerminen³, Markku Kulmala³, Yuesi Wang^{1,2,6}

¹ Institute of Atmospheric Physics, Chinese Academy of Sciences, Beijing 100029, China

² University of the Chinese Academy of Sciences, Beijing 100049, China

³ Institute for Atmospheric and Earth System Research / Physics, Faculty of Science, P.O.Box 64, 00014 University of Helsinki, Helsinki, Finland

⁴ State Joint Key Laboratory of Environmental Simulation and Pollution Control, College of Environmental Sciences and Engineering, Peking University, Beijing 100871, China

⁵ Department of Environmental Science and Engineering, Beijing University of Chemical Technology, Beijing 10029, China

⁶ Center for Excellence in Regional Atmospheric Environment, Institute of Urban Environment, Chinese Academy of Sciences, Xiamen 361021, China

Submitted to Atmospheric Chemistry and Physics

Corresponding to: Yonghong Wang, yonghong.wang@helsinki.fi;

[Yuesi Wang, wys@mail.iap.ac.cn](mailto:Yuesi.Wang.wys@mail.iap.ac.cn)

:

Figure captions

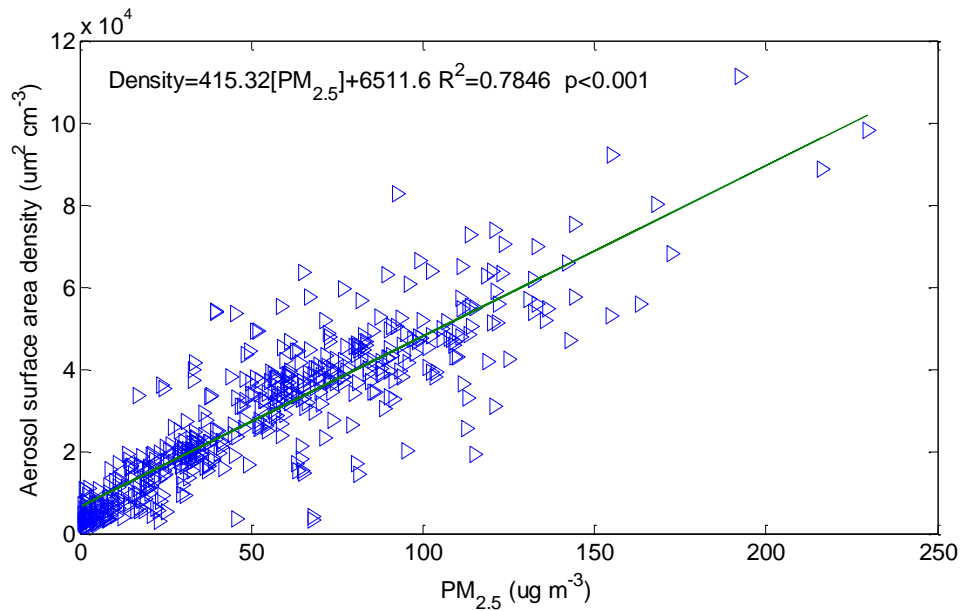


Figure S1. Correlations between aerosol surface area density and PM_{2.5} measured from 1 to 22 November 2018. The green solid line is the regression line.

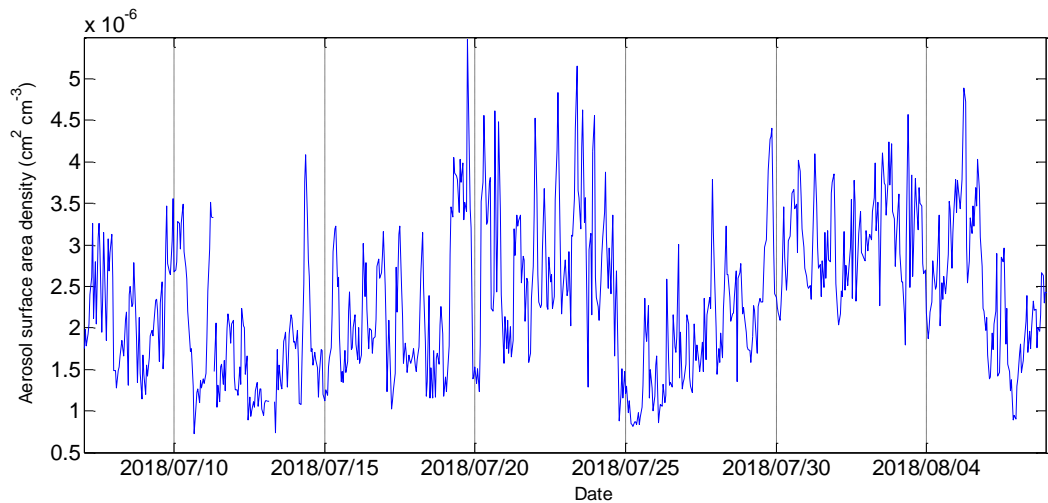


Figure S2. Time series of calculated aerosol surface area density ($\text{cm}^2 \text{cm}^{-3}$) at a suburban site of Xianghe.

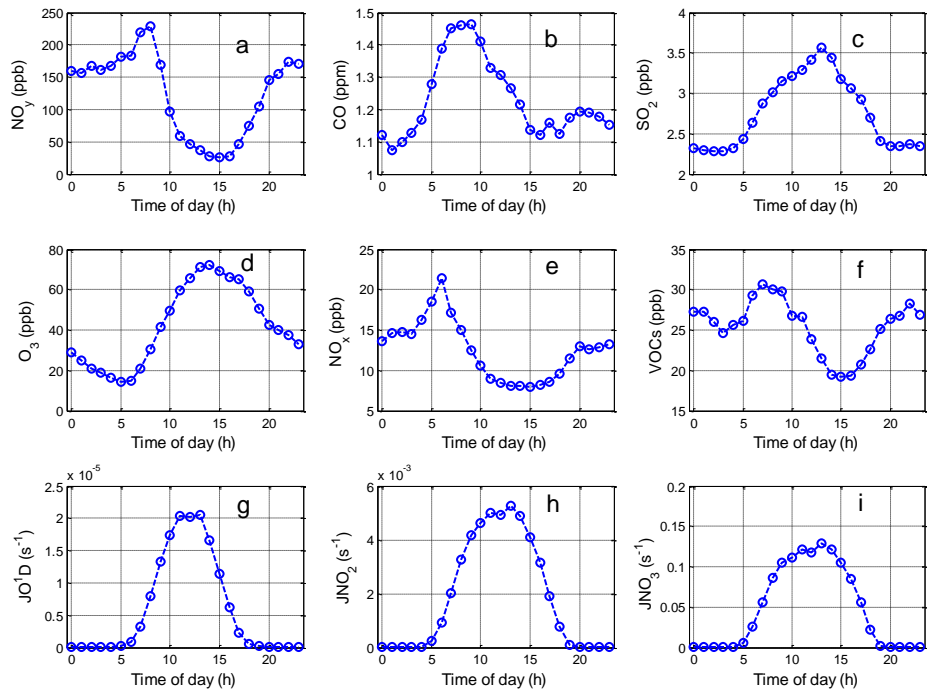


Figure S3. Mean diurnal variations of air pollutants and meteorological parameters observed during the field campaign at Xianghe from 6 July to 6 August 2018.

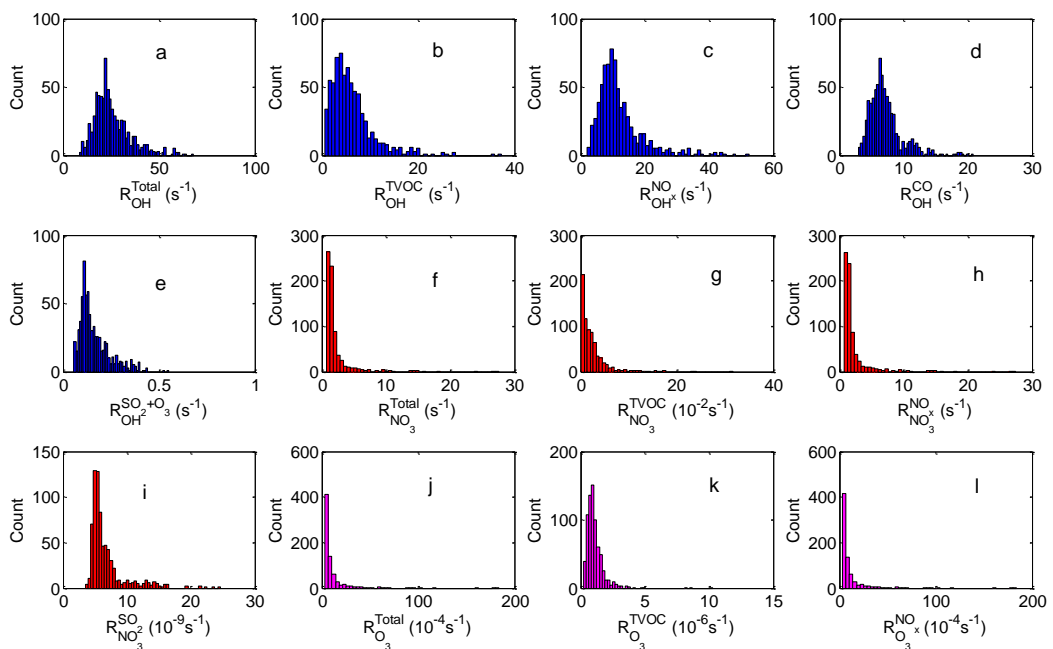


Figure S4. Frequency distributions of $R_{OH}^{calculated}$, $R_{NO_3}^{calculated}$ and $R_{O_3}^{calculated}$ of trace gases during the field campaign at Xianghe from 6 July to 6 August 2018.

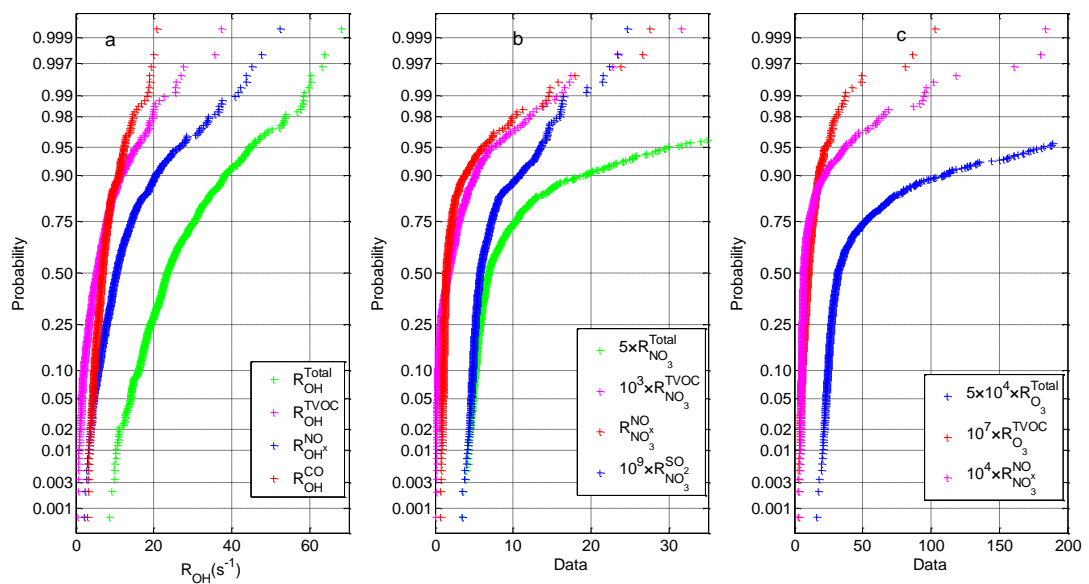


Figure S5. Cumulative frequency distributions of $R_{OH}^{calculated}$, $R_{NO_3}^{calculated}$ and $R_{O_3}^{calculated}$ of trace gases during the field campaign at Xianghe from 6 July to 6 August 2018.

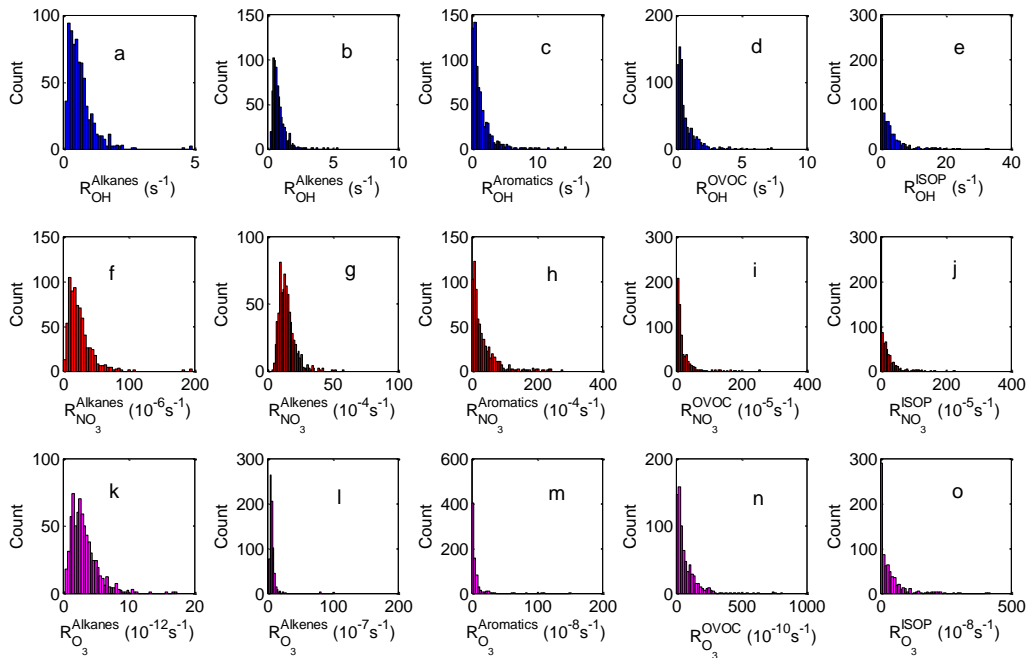


Figure S6. Frequency distributions of $R_{OH}^{\text{calculated}}$, $R_{NO_3}^{\text{calculated}}$ and $R_{O_3}^{\text{calculated}}$ of VOC groups during the field campaign at Xianghe from 6 July to 6 August 2018.

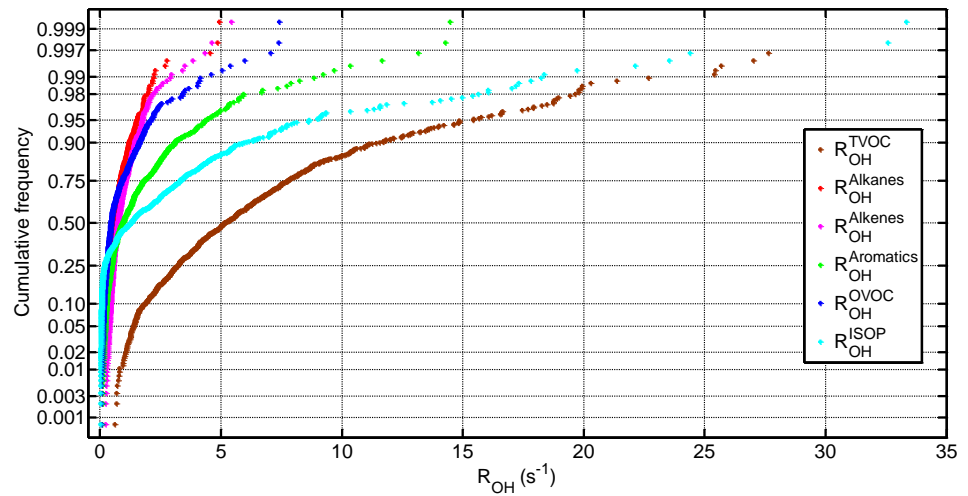


Figure S7. Cumulative frequency distributions of $R_{OH}^{calculated}$ of VOC groups during the field campaign at Xianghe from 6 July to 6 August 2018.

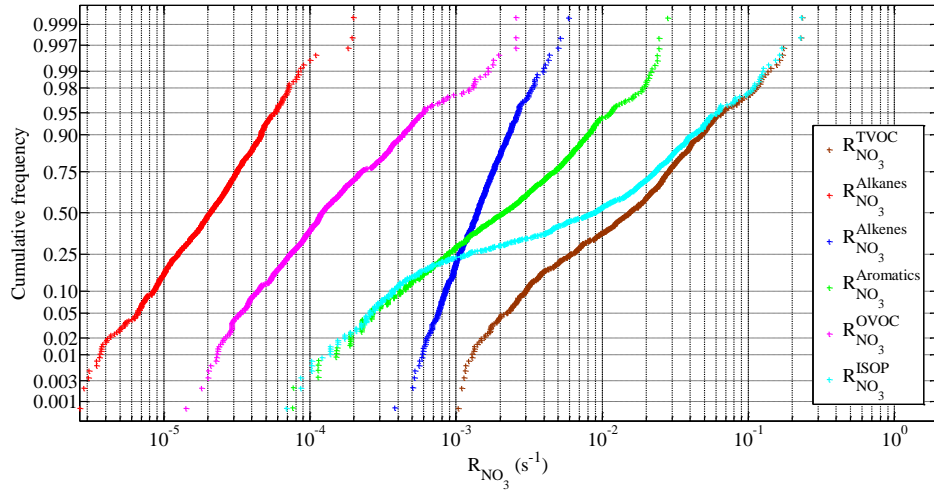


Figure S8. Cumulative frequency distributions of $R_{NO_3}^{\text{calculated}}$ of VOC groups during the field campaign at Xianghe from 6 July to 6 August 2018.

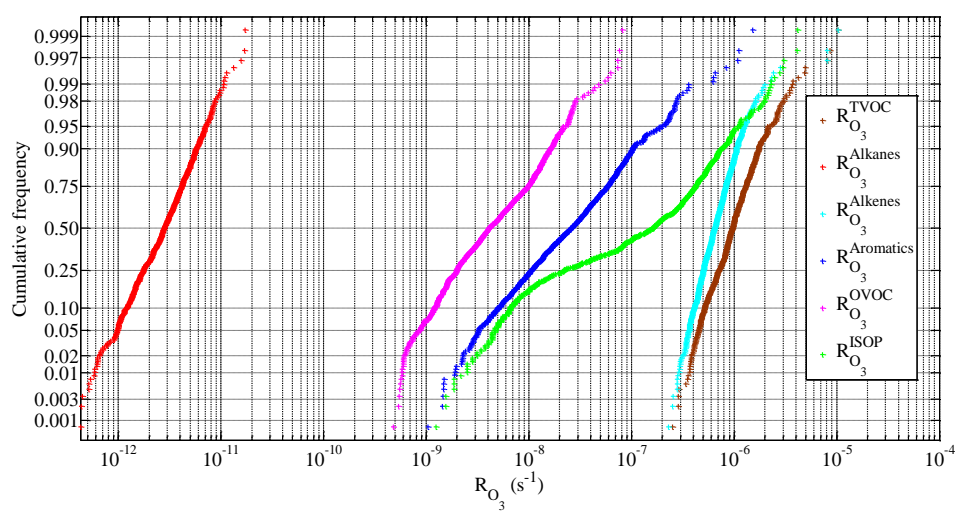


Figure S9. Cumulative frequency distributions of $R_{O_3}^{\text{calculated}}$ of VOC groups during the field campaign at Xianghe from 6 July to 6 August 2018.

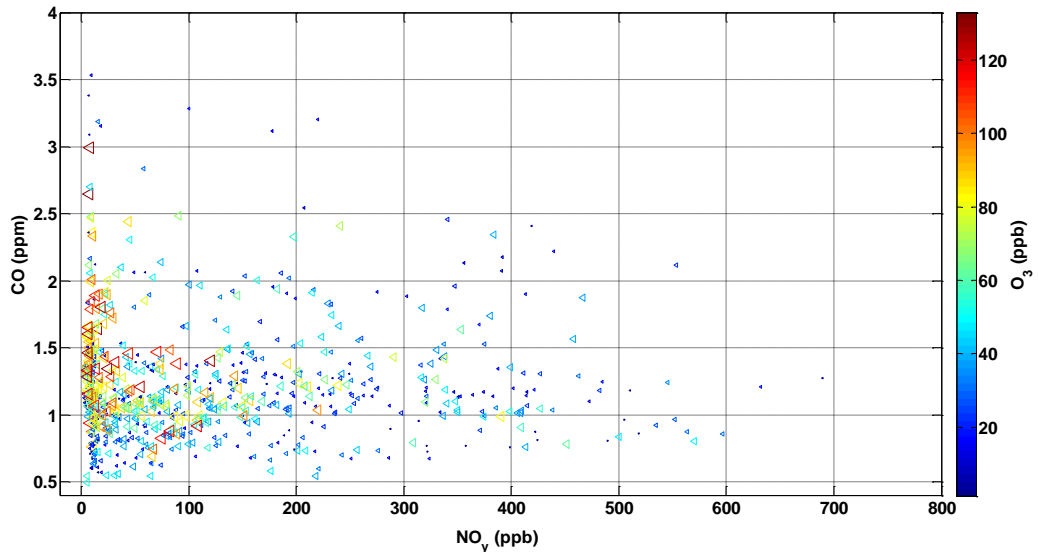


Figure S10. Scatter plots of CO-NO_y color-coded with O₃ concentrations. It shows that high O₃ levels are generally associated with air masses of high CO/NO_y ratio. As VOCs generally have good correlations with CO and play a similar role as CO in photochemical ozone production, the O₃-CO-NO_y relationship strongly indicates a VOC-limited regime of O₃ formation in Xianghe.

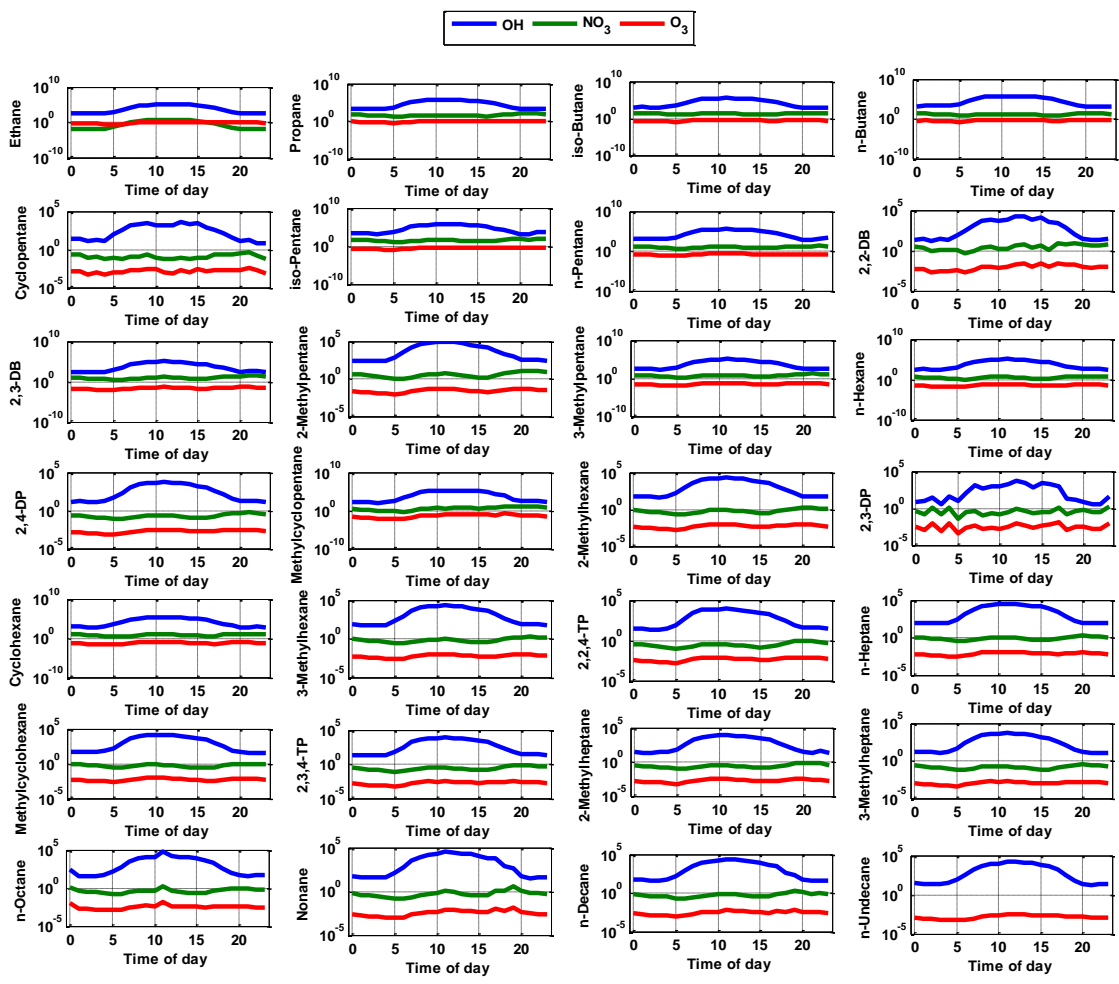


Figure S11. Diurnal variations of alkane species due to the reactions with OH radical (blue lines), NO₃ radical (green lines) and O₃ (red lines) (unit: molecules cm⁻³ s⁻¹). 2,2-DB: 2,2-Dimethylbutane; 2,3-DB: 2,3-Dimethylbutane; 2,4-DP: 2,4-Dimethylpentane; 2,3-DP: 2,3-Dimethylpentane; 2,2,4-TP: 2,2,4-Trimethylpentane; 2,3,4-TP: 2,3,4-Trimethylpentane.

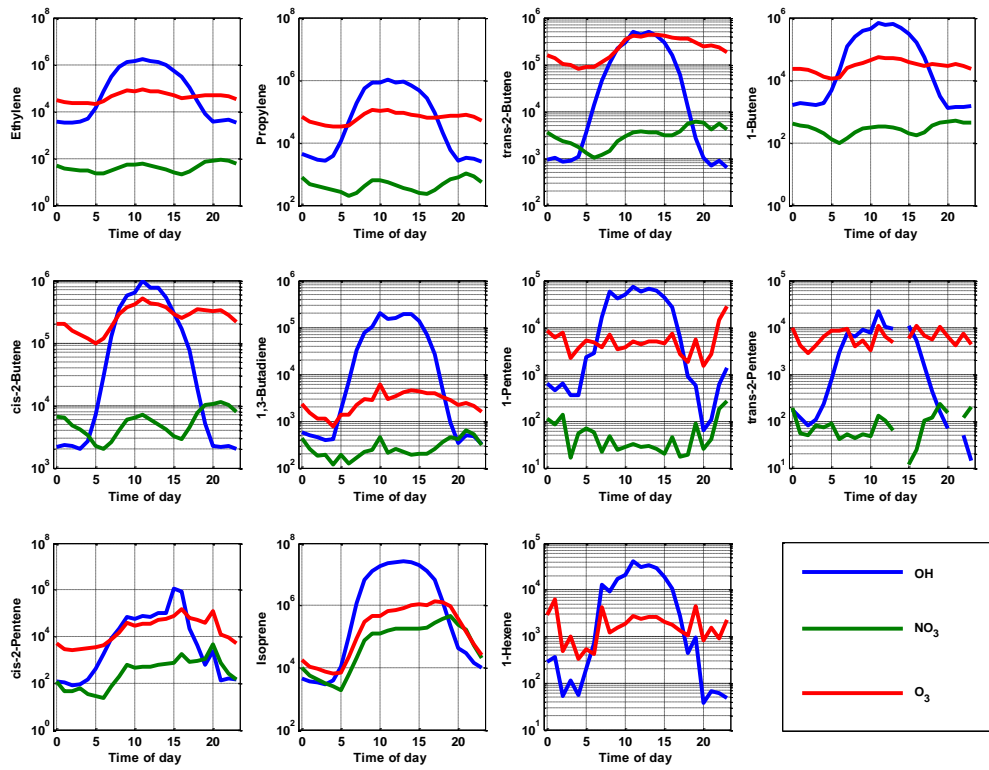


Figure S12. Diurnal variations of alkene species due to the reactions with OH radical (blue lines), NO_3 radical (green lines) and O_3 (red lines) (unit: molecules $\text{cm}^{-3} \text{ s}^{-1}$).

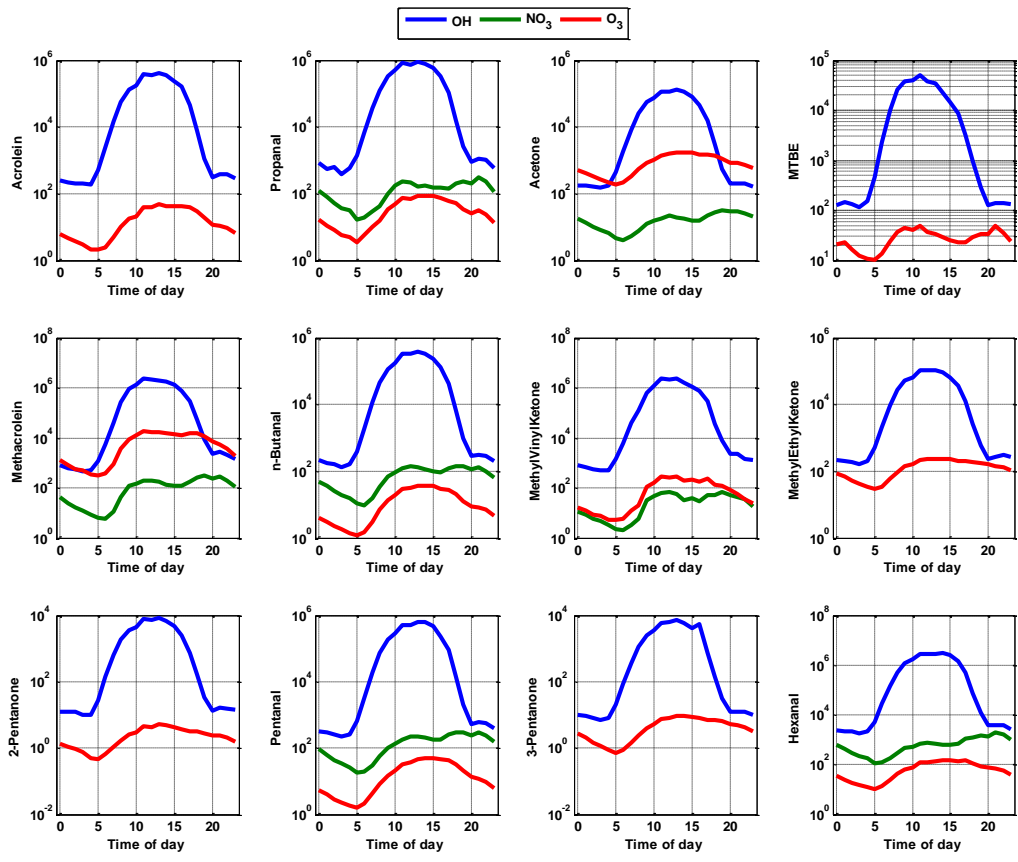


Figure S13. Diurnal variations of OVOC species due to the reactions with OH radical (blue lines), NO₃ radical (green lines) and O₃ (red lines) (unit: molecules cm⁻³ s⁻¹).

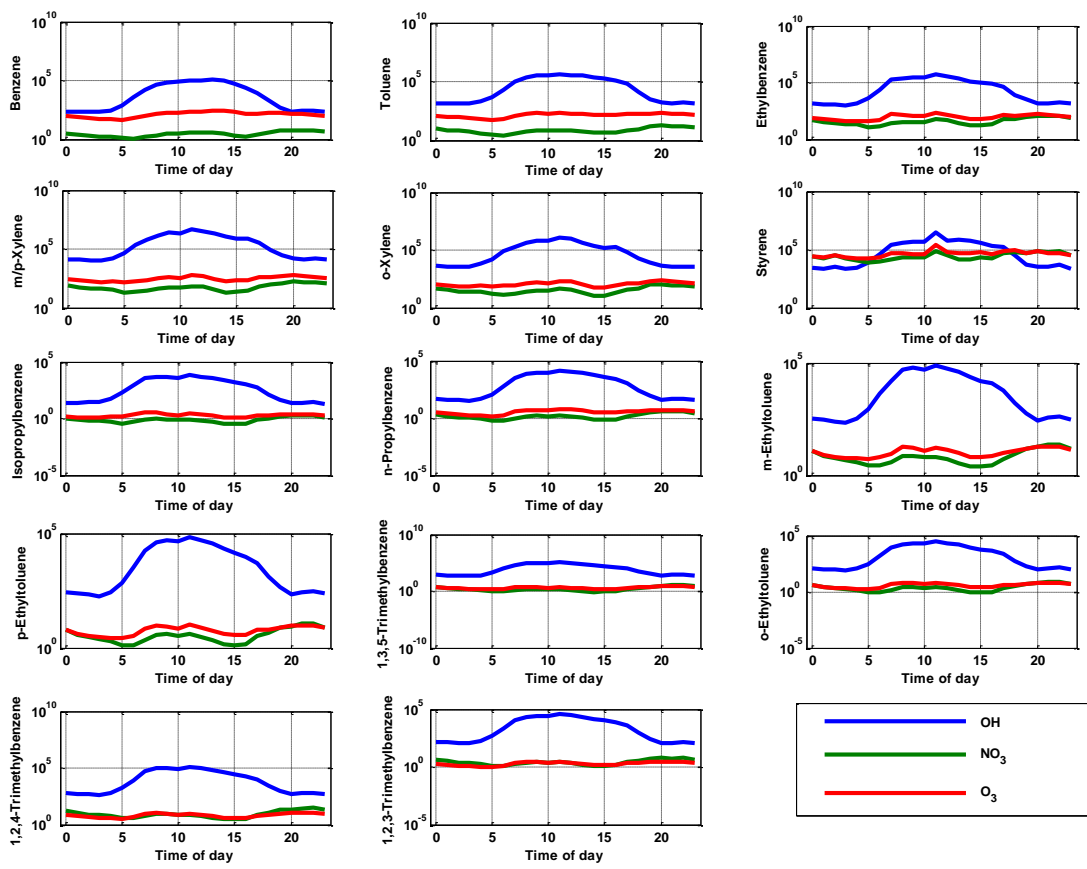


Figure S14. Diurnal variations of aromatic species due to the reactions with OH radical (blue lines), NO_3 radical (green lines) and O_3 (red lines) (unit: molecules $\text{cm}^{-3} \text{s}^{-1}$).

Table captions

Table S1. VOC species for the calculation of R_{OH} , R_{NO_3} and R_{O_3} in this study.

VOCs groups	Species included
Alkanes	Ethane, propane, iso-butane, n-butane, cyclopentane, iso-pentane, n-pentane, 2,2-dimethylbutane, 2,3-dimethylbutane, 2-methylpentane, 3-methylpentane, n-hexane, 2,4-dimethylpentane, methylcyclopentane, 2-methylhexane, 2,3-dimethylpentane, cyclohexane, 3-methylhexane, 2,2,4-trimethylpentane, n-heptane, methylcyclohexane, 2,3,4-trimethylpentane, 2-methylheptane, 3-methylheptane, n-octane, nonane, n-decane, n-undecane
Alkenes	Ethylene, propylene, trans-2-butene, 1-butene, cis-2-butene, 1,3-butadiene, 1-pentene, trans-2-pentene, cis-2-pentene, 1-hexene
Aromatics	Benzene, toluene, ethylbenzene, m/p-xylene, o-xylene, styrene, isopropylbenzene, n-propylbenzene, m-ethyltoluene, p-ethyltoluene, o-ethyltoluene, 1,3,5-trimethylbenzene, 1,2,4-trimethylbenzene, 1,2,3-trimethylbenzene.
O VOCs	Acrolein, propanal, acetone, MTBE, methacrolein, n-butanal, methylvinylketone, methylethylketone, 2-pentanone, pentanal, 3-pantanone, hexanal
Isoprene	Isoprene